View Article Online
View Journal

NJC

Accepted Manuscript

NJC
New Journal of Chemistry
An international journal of the chemical sciences
www.rsc.org/njc
Volume 34 | Number 12 | December 2010 | Pages 2685–3016
ISSN 1144-0546
RSC Publishing
PERSPECTIVE
Kaisa Helttunen and
Patrick Shahgaldian
Self-assembly of amphiphilic
calixarenes and resorcinarenes in water
1144-0546(2010)34:12;1-1

This is an *Accepted Manuscript*, which has been through the RSC Publishing peer review process and has been accepted for publication.

Accepted Manuscripts are published online shortly after acceptance, which is prior to technical editing, formatting and proof reading. This free service from RSC Publishing allows authors to make their results available to the community, in citable form, before publication of the edited article. This *Accepted Manuscript* will be replaced by the edited and formatted *Advance Article* as soon as this is available.

To cite this manuscript please use its permanent Digital Object Identifier (DOI®), which is identical for all formats of publication.

More information about *Accepted Manuscripts* can be found in the **Information for Authors**.

Please note that technical editing may introduce minor changes to the text and/or graphics contained in the manuscript submitted by the author(s) which may alter content, and that the standard **Terms & Conditions** and the **ethical guidelines** that apply to the journal are still applicable. In no event shall the RSC be held responsible for any errors or omissions in these *Accepted Manuscript* manuscripts or any consequences arising from the use of any information contained in them.

RSC Publishing

www.rsc.org/njc
Registered Charity Number 207890

Graphical abstract

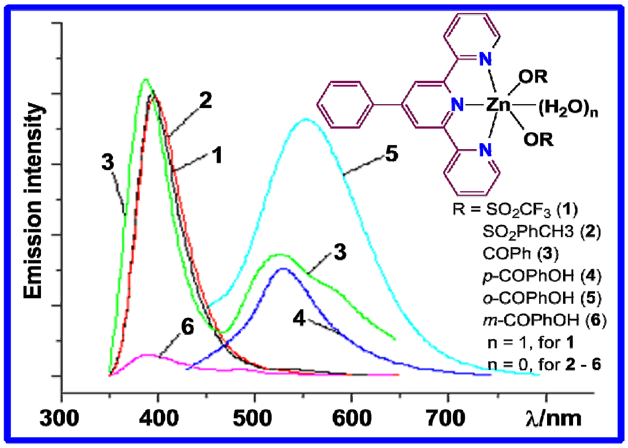

The zinc(II) mononuclear complexes [Zn(OR)$_2$L] were obtained by reaction of several zinc salts (trifluoromethane sulfonate, *p*-toluenesulfonate, benzoate and *p*-, *o*-and *m*-derivatives) with 4′-phenyl-terpyridine (L). Their photoluminescent and thermal properties were studied.

Synthesis, Characterization, Photoluminescent and Thermal Properties of Zinc(II) 4′-phenyl-terpyridine Compounds

Zhen Ma [a,b]*, Wanbing Lu [a], Baohuan Liang [a] and Armando J.L. Pombeiro [b]*

[a] Guangxi Key Laboratory of Petrochemical Resource Processing and Process Intensification Technology, School of Chemistry and Chemical Engineering, Guangxi University, Nanning 530004, P. R. China; E-mail: mzmz2009@sohu.com

[b] Centro de Química Estrutural, Complexo I, Instituto Superior Técnico, Technical University of Lisbon, Av. Rovisco Pais, 1049-001, Lisbon, Portugal, E-mail: pombeiro@ist.utl.pt

Abstract

Reactions between 4′-phenyl-terpyridine (L) and several Zn(II) salts (trifluoromethane sulfonate, *p*-toluenesulfonate, benzoinate, *p*-hydroxybenzoinate, *o*-hydroxybenzoinate or *m*-hydroxybenzoinate) led to the formation of the complexes $[Zn(OSO_2CF_3)_2L(H_2O)]$ (**1**), $[Zn(p\text{-}OSO_2PhCH_3)_2L]$ (**2**), $[Zn(OCOPh)_2L]$ (**3**), $[Zn(p\text{-}OCOPhOH)_2L]$ (**4**), $[Zn(o\text{-}OCOPhOH)_2L]$ (**5**) and $[Zn(m\text{-}OCOPhOH)_2L]$ (**6**), which were characterized by elemental analysis, ^{1}H NMR, ^{13}C NMR, IR, single crystal X-ray diffraction and fluorescence spectroscopies. In **1**, the Zn atom is hexacoordinated, with a N_3O_3 coordination environment, whereas in the remaining structures the metal atom is envisaged as possessing distorted N_3O_2 irregular trigonal bipyramidal coordination geometries. All the compounds show interesting photo-luminescent properties in solid and solution states in DMF, DMSO and methanol, which are reported along with their TG-DTA thermal decomposition processes.

Introduction

Characterized by featuring three distinct pyridyl groups, terpyridine ligands behave as suitable hosts for transition metal ions.[1-17] They provide impetus for chemists to design a large number of coordination compounds for use in many fields, namely in material and medicinal chemistries.[9-16] Since the work of Constable *et al.*, many new terpyridine compounds, which show special coordinative abilities towards transition metal elements, have been synthesized by condensation of the respective aldehydes and 2-acetonepyridine followed by oxidation, in simple and high yield processes.[18-22] Other terpyridine-like ligands were also reported.[23] Combining these ligands with transition metal ions leads to a diversity of complexes with interesting properties,[1-22] in particular showing photoluminescence [12,13,16] and antitumor activities.[16a] For the general [n:n] type of terpyridine compounds (mainly 2:2 or 1:1), the photoluminescence and antitumor activities are known to depend not only on the terpyridine ligands and metal ion, but also on the anionic co-ligands and counterions. Hence, to investigate the effects of the auxiliary ligands on the structural and photo-luminescent properties of zinc terpyridine complexes, we synthesized a series of six novel complexes of this metal with a multi-pyridyl ligand (4′-phenyl-terpyridine), and bearing, as anionic ligands, trifluoromethane sulfonate ($OSO_2CF_3^-$), p-tolylsulfonate (p-$CH_3PhSO_3^-$), benzoate ($PhCOO^-$), or *p*-, *o*, *m*-hydroxyl substituted benzoate. They were characterized by elemental analysis, NMR, IR, X-ray structural analysis, and their photoluminescence in solid state or solutions of DMF, DMSO and methanol was studied.

2. Results and discussion

2.1. Syntheses and characterization of the complexes

4′-phenyl-terpyridine (L) was obtained according to a literature procedure, [17] and the Zn(II) complexes $[Zn(OSO_2CF_3)_2L(H_2O)]$ (**1**), $[Zn(p\text{-}OSO_2PhCH_3)_2L]$ (**2**), $[Zn(OCOPh)_2L]$ (**3**), $[Zn(p\text{-}OCOPhOH)_2L]$ (**4**), $[Zn(o\text{-}OCOPhOH)_2L]$ (**5**) and $[Zn(m\text{-}OCOPhOH)_2L]$ (**6**) were synthesized (Scheme 1) by reaction of L with the appropriate Zn(II) salt added in stoichiometric amounts, i.e. $Zn(SO_3CF_3)_2$, $Zn(p\text{-}SO_3PhCH_3)_2\cdot 6H_2O$, $Zn(OCOPh)_2$, $Zn(p\text{-}OCOPhOH)_2\cdot 3MeOH\cdot 1.5H_2O$, $Zn(o\text{-}OCOPhOH)_2\cdot 2H_2O$ or $Zn(m\text{-}OCOPhOH)_2\cdot 2H_2O$, respectively, in a methanol - CH_2Cl_2 solution. The reactions usually proceeded smoothly at room temperature and the complexes were isolated after 24 h, in good to high yields (50 – 90 %). In the case of **3**, the conditions were harsher (hydrothermal synthesis at 120 °C for two days).

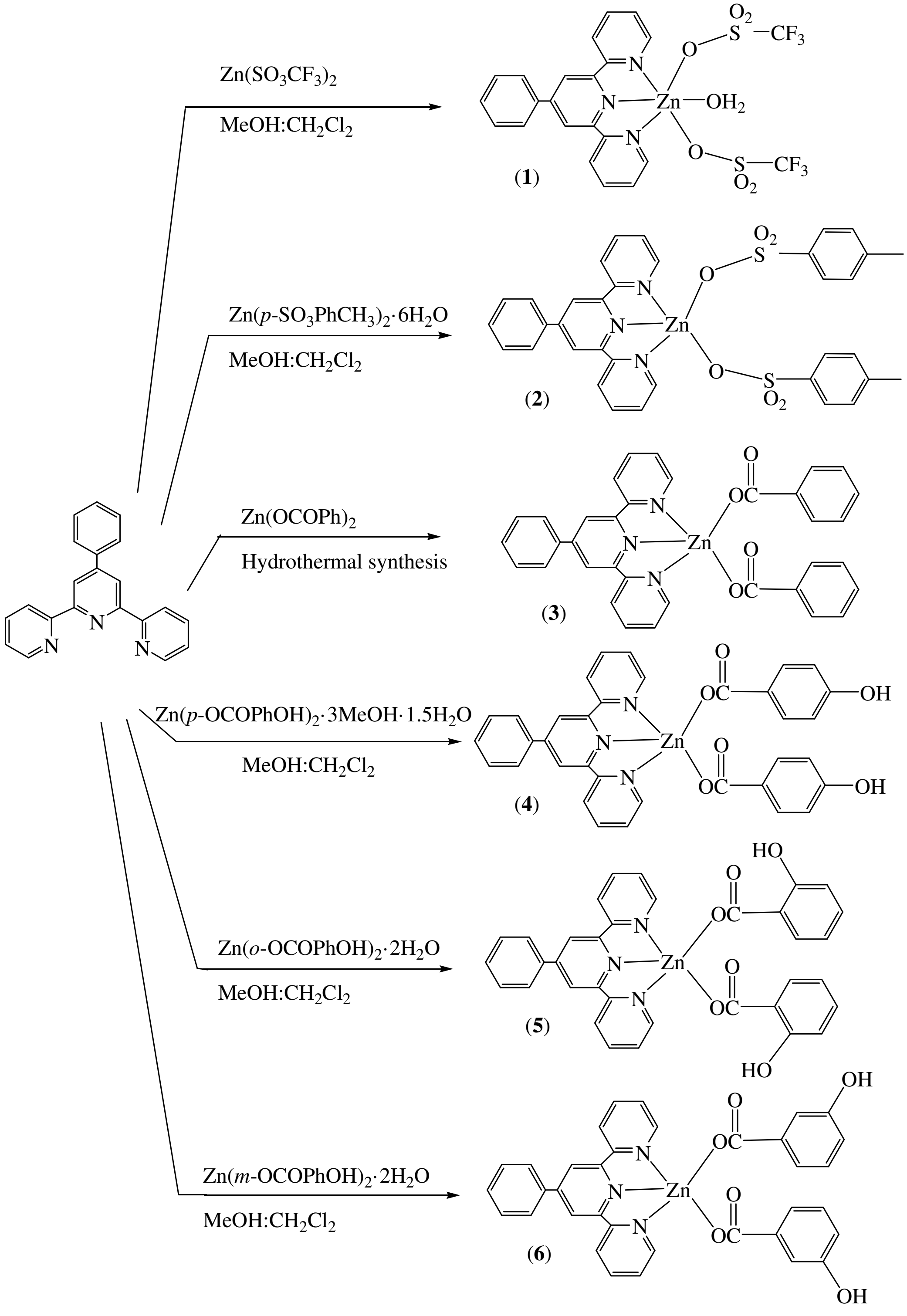

Scheme 1

2.2. Elucidation of the structures of the compounds

The six complexes were isolated as white solids which were characterized (see experimental) by elemental analysis, ^{1}H NMR, ^{13}C NMR (*e.g.*, the protons of the –OH group in **4**, **5** and **6** resonate at δ 9.79, 13.22 and 9.34, respectively, whereas the carboxylate carbons of the corresponding ligands appear at δ 170.5 – 173.1), IR and fluorescence spectroscopies, as well as by X-ray diffraction. Suitable crystals of all the complexes for X-ray analysis were obtained upon crystallization from methanol solution or the mother liquor solution by diffusion of diethyl ether (**1**, **2**, **4** and **5**), hydrothermal method (**3**) or slow evaporation of the mother liquor solution (**6**). Compound **4** crystallizes with one molecule of methanol.

$[Zn(OSO_2CF_3)_2L(H_2O)]$ **1** is a mononuclear neutral di-trifluoromethanesulfonate complex (Fig. 1). The zinc ion is coordinated with six atoms, three nitrogen atoms from the terpyridine ligand, two oxygen atoms from the two anionic ligands and one oxygen atom from water, involved in a distorted ZnN_3O_3 octahedral geometry with the coordinated oxygen atoms of the two ligated $CF_3SO_3^-$ occupying the apical positions [bond angles range from 83.32(6) to 97.04(6)º between the apical atoms and the equatorial positions]. This type of geometry is that usually reported for related Zn(II) compounds, *e.g.* $[Zn_2(\mu\text{-}O_2SO_2)_2L_2(CH_3OH)_2]$ (L = 4′-phenyl-2,2’:6’,2”-terpyridyl),[16a] or $[Zn(OSO_2CF_3)_2L(H_2O)]$ [L = 12,12- dimethyl-7,10,14,17-tetraoxa-1(3,6),3(2,5),2(2,6)- tripyridina--11,13(1,4)-dibenzenacycloicosaphane].[24] Several intermolecular hydrogen bonds exist in the structure, and two of them are worth to be mentioned. They involve the coordinated water molecule and the O2 and O6 oxygen atoms from the two $CF_3SO_3^-$ ligands, along with several others involving the other oxygen atoms or a fluorine atom of $CF_3SO_3^-$ with hydrogen atoms at the carbon atoms of phenyl or pyridyl groups of the terpyridine ligand. In its structure, the terpy group in the ligand is nearly planar (with an RMS deviation of 0.0585 Å). Moreover, the phenyl ring is twisted (17.82(14)º) with the connecting pyridyl or (20.08(12)º) relative to the plane containing N1, N2, N3 and Zn1. Due to the position and orientation of the trifluoromethanesulfonate in **1**, the Zn complex molecules are too far apart for any convenient π-π interaction, a situation that contrasts with the structures of other terpyridine-type complexes.[12,16] However, several π-ring interactions (Y-X...Cg) exist in the structure, within the range of 3.039 - 3.762 Å.

The asymmetric unit of compound **2** (Fig. 2) comprises half of the molecule because of the symmetry of the compound. The mononuclear complex crystallized in a centrosymmetric space group and the atoms Zn1, N2, C8, C9 and C12 are located on the twofold axis. Each zinc ion is coordinated by the three N atoms of the 4′-Ph-terpy (L) ligand and two oxygen atoms from two

$SO_3PhCH_3^-$ ions, therefore forming an irregular N_3O_2 trigonal bipyramidal coordination environment (Fig. 2). The three pyridyl units of the ligand are almost perfectly flat (with an RMS deviation of 0.0225 Å) and the phenyl group in complex **2** is folded and twisted, as revealed by the angle between the phenyl ring and the connected pyridyl (18.57(7)º) and the plane formed by Zn, N1, N2 N1A (16.47(6)º). The Zn1─N2 bond distance of 2.052(2) Å for the central pyridyl ring is shorter than that for the terminal ones, Zn1─N1 and Zn1─N1A bonds [2.1570(19), 2.1570(19) Å, respectively], what is also shown by all the complexes of this study. The structure presents no intermolecular π-π interactions but two π-ring (Y-X...Cg) interactions between two oxygen atoms at the sulfonates and two neighbouring rings constituted by Zn1-N1-C5-C6-N2 with an atom-centroid distance (X..Cg) of 3.5076 Å. Further stabilization, by several intermolecular hydrogen bonds, can also be found, involving the O2 sulfonate oxygen and the hydrogens at carbon atoms of the ligand, although no classic hydrogen bond is present in the structure.

Like **2**, compounds **3**, **4**, **5** and **6** (Figs. 3 - 6) are also mononuclear species crystallized in centrosymmetric space groups. The asymmetric units of the compounds present half of the molecule in **3** and **6**, one molecule in **4**, and two molecules in **5**, respectively, because of the symmetry of the molecule. The atoms Zn1, N2, C8, C9 and C12 are also located on the twofold axis in **3** and **6**. The coordination environment around the zinc ion in these compounds displays an irregular trigonal bipyramidal geometry, as in complex **2** and other related compounds [12, 16], which results from the coordination of zinc by three nitrogen atoms from the terpyridine ligand and two oxygen atoms from the auxiliary ligands in a monodentate mode. The average contacts between the central metal ion and the oxygen atoms (Zn–O) is 1.957 Å in **3**, which has no hydroxyl group at its auxiliary ligands, being shorter than those in **4** (1.984 Å), **5** (1.974 Å) and **6** (1.971 Å). This is indicative that the hydroxyl substituent has an elongating effect on the Zn-O bond lengths. However, these bond lengths do not follow the sequence of pK_a values of the conjugated acids of the anions, the latter being 2.98 (for *o*-), 4.08 (for *m*-), 4.17 (for benzoic acid) and 4.58 (for *p*-hydroxyl benzoic acid). Such bond lengths are not only affected by the basicity of the anions but also by other factors, including hydrogen bonds, or even spatial environments determined by the positions of the hydroxyl groups at the phenyl rings.

The three pyridyl units of L in these complexes are planar (with an RMS deviation of 0.0668 Å for **3**, 0.1685 Å for **4**, 0.0741 and 0.0527 Å in **5**, and 0.0185 Å in **6**). The angles between the pendent phenyl rings and the connected pyridyls and the attached N-N-N-Zn planes are 18.97 (9) and

21.08(9)° in **3**, 33.81(11) and 36.91(11)° in **4**, 9.02° (3.81(6)° in one molecule and 14.23(5)° in the other) and 11.00° (7.50(7) and 14.50(7)° for the respective two molecules) in **5**, and 5.82(15) and 4.81(15)° in **6**, respectively, showing that there is not a great effect of the hydroxyl substituent on these angles. No classic hydrogen bond is found in the structure of **3** but two other kinds of intermolecular hydrogen bonds can be found in the structure, involving the O2 oxygen of the benzoate and the hydrogens at carbon atoms of the terpyridine ligand. Intermolecular hydrogen bonds exist in the structures of **4**, **5**, and **6**, which are in the range of 2.50 – 3.50 Å. Unlike **4** and **6**, which only shows intermolecular hydrogen bonds, intramolecular hydrogen bonds also exist in the structure of **5** because of the *ortho*-position of the hydroxyl substituent, thus further consolidating the structure.

Several π-ring interactions exist in each structure of the complexes between oxygen or H atoms and their neighbouring rings. The structure of **3** presents two kinds of π-ring (Y-X...Cg) interactions: one is between one hydrogen at C3 and a neighbouring phenyl ring of a benzoate with an atom-centroid distance (X..Cg) of 2.660 Å; the other one is between one oxygen atom (O2) of a benzoate and two neighbouring rings constituted by Zn1-N1-C5-C6-N2 or by Zn1-N2-C6-C5A-N1A with the atom-centroid distances (X…Cg) of 3.398 and 3.398 Å, respectively. In **4**, several π-ring interactions are present (Y-X...Cg is 2.868 Å and H-X...Cg are in the range of 2.74 – 2.95 Å) between one oxygen atom (O2) at a benzoate ligand or several H atoms and their neighbouring rings, which are in the range of 2.79 – 2.96 Å for X-H...Cg and 3.076 – 3.333 Å for Y-X...Cg in **5**, and 3.039 – 3.763 Å for Y-X...Cg in **6**.

2.3. TG-DTA properties of the complexes

The TG properties of the six complexes were studied and the results for the sulfonated compounds **1** and **2** are shown in Fig 7, whereas the others are deposited as supporting material.

Fig. 7(a) shows the TG and DTA curves for complex **1**. There are three major decomposition steps corresponding to loss of the solvent and two decomposition processes of the molecules. The first loss is in the range of 139-185 °C (centred at 162 °C) and it concerns the loss of the coordinated water molecule. The weight loss in this step is 2.51 % (calc. 2.61 %). The second decomposition occurs in the temperature range of 369 - 541 °C (centred at 455 °C) and corresponds to a 45.5 % loss of weight. The loss in the final decomposition process is 8.88 mg within the temperature range of

541 – 743 °C (centred at 642 °C) with the percentage of 38.8 %. The final product is ZnO and its weight is 2.99 mg with the percentage of 13.1, which matches with the calculated value of 11.8 %.

The TG and DTA curves of compound **2** are shown in Fig. 7(b). It has three major weight losses corresponding to a gradual loss of two methyl groups and two decomposition steps. The first loss, in the range of 180 – 306 °C (centred at 243 °C) can possibly be accounted for by the loss of the two methyl groups at the two *p*-toluene sulfonate ligands. The total loss is 3.80 % (calc. 4.19 %). The second decomposition step is in the range of 389 – 507 °C (centred at 448 °C) and the total loss is 21.5 %, and the next one occurs in the range of 507 - 891 °C (centred at 699 °C). The percentage of lost weight in this step is 61.2 %. The final product is ZnO and its percentage is 13.0 %, which is comparable to the calc. value of 11.4 %. The results show that compound **2** is more thermal stable than **1.** The final stable temperature in the case of **2** is 891 °C, much higher than that (743 °C) of **1**. The decomposition processes for the two compounds are different. By comparison with the thermal decompositions of $ZnSO_4 \cdot 7H_2O$ and a Zn cyclic dithiocarbamate compound,[25, 26] complex **2** appears to lead to the formation of $ZnSO_4$ and then ZnO, whereas **1** undergoes conversion to [ZnOL] on the way to ZnO.

The TG-DTA properties of the benzoate complexes **3**, **4**, **5** and **6** were also studied and their decomposition processes are summarized in Table 2. The final product of thermal decomposition of the four complexes is also ZnO, what corresponds to 14.1 % for **3**, 11.2 % for **4**, 13.7 % for **5** and 13.2 % for **6**, complying with the theoretical value of 13.2 % (**3**), 11.8 % (**4**), 12.5 % (**5**), and 12.5 % (**6**), respectively.

The results are indicative that the decomposition processes and the final stable temperatures greatly depend on the auxiliary ligands. In comparison with complexes **1** and **2** bearing the substituted sulfonate ligands, the final stable temperatures of the benzoate complexes **3** - **6** are lower. Complex **4**, with the hydroxyl substituent in *para* position, displays the lowest final state temperature (491 °C), being easier to decompose than the others. Complex **6**, with the *meta*-OH substituent, is the benzoate complex with the highest final state temperature (700 °C). Differences in hydrogen-bonds (which in the case of the *ortho*-OH complex **5** can be intramolecular) are expected to play a role in the decomposition processes.

Table 2 Decomposition processes in TG-DTA of the benzoate complexes **3 - 6**

Complex		**3**	**4**	**5**	**6**
Step 1	a, °C	322 – 428	70-106	275 – 321	333-405
	b, %	59.8	4.80	21.7	27.9
Step 2	a, °C	463 – 651	260 – 341	349 – 383	431 – 528
	b, %	26.1	23.2	12.4	28.8
Step 3	a, °C		376 – 458	383 - 420	528 – 700
	b, %		52.6	8.0	30.0
Step 4	a, °C		458 – 491	420 - 655	
	b, %		8.2	32.9	

a. Temperature range of decomposition in TG-DTA of the complex;

b. Percentage of weight loss in every decomposition process of the complex.

2.4. Photoluminescent properties

All the compounds **1** – **6** show interesting photoluminescent properties in the solid state at room temperature, and their emission spectra are presented in Fig 8. The sulfonate compounds **1** and **2** show very strong photoluminescent bands in their spectra (the determinations were run with a small amount of samples, a few mg, and under conditions of the narrowest slits of emission and excitation, see experimental section). Compound **1**, excited at 300 nm, has one band in its emission spectra at *ca.* 394 nm, which is similar to the photoluminescent band in the emission spectrum of compound **2** (excited at 300 nm), which appears at *ca.* 386 nm. These results are indicative that the organic parts of the sulfonate ligands have no marked effects on the photoluminescence of the complexes. In comparison with the already reported photoluminescence of the free ligand L,[13] the bands of **1** and **2** can tentatively be assigned to an intraligand charge transfer (ILCT).

In the benzoate complex **3**, two bands are clearly detected, one at 387 nm with a high intensity and the other at 524 nm with a medium intensity. A related zinc complex bearing acetate instead of benzoate displays two bands in its photoluminescent spectrum at 381 (high intensity) and 500 nm (low intensity) [16a]. The first peaks, at the higher energy, are very close and with similar intensity (also for complex **1**), being assigned (see above) to an ILCT band. The second peaks differ by 24 nm for the benzoate (**3**) and acetate complexes. This is attributed mainly to the different electronic properties of their anionic ligands. The phenyl group at benzoate has a positive induction effect, whereas the methyl group at acetate has a negative one, and the band undergoes a blue-shift from 524 to 500 nm, being tentatively assigned to a MLCT band. [27, 28]

The benzoate compounds **4**, **5** and **6**, with the hydroxyl substituent, show also interesting photoluminescent properties, the positions and intensities of their bands depending on the position of the hydroxyl group at the benzoate ligand. In the spectrum of **4**, excited at 390 nm, a band with medium intensity is observed at 530 nm, whereas a strong peak at 553 nm is displayed by the spectrum of **5**. When excited at 300 nm, both compounds show their emission bands at 413 and 411nm, respectively. As for the complexes **1** and **2**, the band is assigned to a MLCT. [12,16,27,28] It is an interesting result that the band at ca. 390 nm, observed in **1**-**3** and in some Zn and Cd 4′-phenyl-terpyridine compounds,[12,16] is not exhibited by **4** and **5**. The behaviour of **6** is unique in comparison with **4** and **5**, since the peak at 390 nm is observed, although with a very low intensity. However, a clear rationale for the overall effect of the position of the hydroxyl substituent in the phenyl ring cannot be established, conceivably depending on inductive and resonance effects, hydrogen bonds, interaction with the neighbouring molecules or packing of the molecules in the solid state. The bands of photoluminescence in these compounds do not follow the sequence of pK_a values of the conjugated acids of the anions. Although compound **5**, bearing the carboxylate ligand with the lowest pK_a value of the conjugated acid, shows the lowest energy of the emission band, the other compounds do not follow such a sequence.

The photoluminescent properties of the complexes were also studied in solution. On account of their solubility in DMSO, DMF and methanol, these were the selected solvents (Table 3).

Table 3 Photoluminescent properties of the complexes in solution

Complex	Bands, nm	DMSO[a]	DMF[a]	Methanol[a]	
1	Ex_{max}	378, 478	379, 478	252	362, 434
	Em_{max}	518	519	366	513
2	Ex_{max}	379, 478	378, 480	252	361, 434
	Em_{max}	443, 513	449, 518	367	513
3[b]	Ex_{max}	375, 479	376, 479	255	
	Em_{max}	443, 508	508	366	
4	Ex_{max}	375, 479	375, 480	300	364, 433
	Em_{max}	512	510	367	509

5	Ex_{max}	376, 479	376, 483	264	365, 434
	Em_{max}	397, 515	512	368	511
6	Ex_{max}	375, 479	375, 480	259	359, 434
	Em_{max}	445, 511	439, 510	366	510

a. The concentrations of the six complexes prepared in the tests are 1 mmol/L in DMSO, and 0.5 mmol/L in DMF and methanol.

b. In a 1:1 mixture of DMSO and methanol, a weak band appears at 438 nm (when **3** is excited at 382 nm) or at 513 nm (when **3** is excited at 371 or 453 nm).

The six complexes show a strong photoluminescence at *ca.* 515 nm both in DMSO and DMF with the two Ex_{max} at *ca.* 378 and 479 nm. **1** and **4** show only one emission band in DMSO and DMF. **2** and **6** display two bands in both solvents. **3** and **5** exhibit two bands in DMSO, but only one in DMF.

In methanol, a new emission band appears at *ca.* 366 nm in the spectra of all the six complexes. Strong emission bands are also observed in methanol at *ca.* 510 nm, except for **3** which does not show such an emission band in this solvent. In a 1:1 solution of DMSO and methanol, complex **3** shows a weak band at 438 nm (when excited at 382 nm) or at 513 nm (when excited at 371 or 453 nm). The results are indicative that DMSO enhances the band at *ca*. 513 nm but quenches the band at *ca.* 365 nm, whereas methanol has the opposite effect. The combined effects of the two solvents results in the appearance of the two weak bands of **3** in their mixture.

From the results obtained in the photoluminescent studies, the three peaks appearing at *ca*. 366, 445 and 515 nm are tentatively assigned to ILCT, LMCT and MLCT, respectively. [12,16,27,28] The results also show that these charge transfers are affected by the anionic auxiliary ligands and the solvents used in the tests.

Conclusion

4′-phenyl-terpyridine appears as a convenient N,N,N-tripodal ligand source towards the easy synthesis of zinc complexes with interesting photoluminescence.

Six Zn(II) complexes with such a ligand were obtained (usually in good yields) by a simple reaction with an appropriate zinc salt, and, in their composition, the auxiliary anionic ligand was determined by the nature of the salt. The zinc complexes thus prepared show photoluminescence in the solid state and in solution (in DMSO, DMF and methanol) at room temperature and the photoluminescent properties (namely the energy and intensity of the emission bands) are markedly dependent on the anionic auxiliary ligands and on the solvents used in the tests. In particular, compounds **1** and **2** show a very strong photoluminescence at the high energy region, indicating that a sulfonate is a much better auxiliary ligand in these terpyridine compounds, concerning the photoluminescent properties, than a carboxylate ligand in that energy region. Moreover, these properties are easily turned upon variation of the organic group of the sulfonate ligand. Within the carboxylate complexes, the position of the hydroxyl group substituent at the aromatic ring also has a marked effect, and, *e.g.*, the *ortho* position (complex **5**) results in an enhancement of the intensity of the low energy band, whereas the *meta* position (complex **6**) does not show that band but enhances the high energy one, in the solid.

The thermal properties of the complexes are also greatly affected by the auxiliary ligands. The sulfonate complexes display a higher final stable temperature than the carboxylate ones. Within the latter, the *meta* position of the hydroxyl group (compound **6**) results in the highest thermal stability.

However, a clear rationale for the overall effect of the position of the hydroxyl substituent in the phenyl ring cannot be established, conceivably depending on inductive and resonance effects, hydrogen bonds interaction with the neighbouring molecules or packing styles of the molecules in the solid state.

Nevertheless, the recognition of the above types of effects can be of significance towards further design of photoluminescent materials. The work provides good candidates for further photoluminescent studies and deserves to be extended to other substituted terpyridine zinc complexes on attempting to study substituent effects and to establish relationships.

3. Experimental

3.1. Instrumentation and reagentes

^{1}H NMR spectra were run on a Varian Unity 400 spectrometer. Elemental analyses were determined with an Elementar Vario EL III Elemental Analyser. IR spectra were measured with a Perkin–Elmer Spectrum 2000 or a Magna750 FT-IR spectrophotometer, in KBr pellets. Emission and excitation spectra were recorded on a Perkin–Elmer LS 55 luminescence spectrometer with a red-sensitive photomultiplier type R928. TG-DTA data were collected with a Perkin Elmer STA6000 Simultaneous Thermal Analyzer at a heating rate of 10 K min^{-1} under an air atmosphere. All reagents used in the experiments were of analytical grade or purified by standard methods. The amounts of the solid state samples used in the photoluminescent studies are as follows: 3 mg for compounds **1** and **2**, and 25 mg for compounds **3** - **6**. For **1** and **2**, the photoluminescent experiments were undertaken with the narrowest slits (2.5) of excitation and emission.

3.2 Synthesis

4′-Ph-terpy (L) was prepared by following a reported procedure.[17] $Zn(SO_3CF_3)_2$ is a product of Fluka. $Zn(OCOPh)_2$ was synthesized by the reaction of $Zn(NO)_2{\cdot}6H_2O$ and NaCOOPh in water. Other salts were prepared by the reaction of $Zn(OH)_2$ and the respective acids.

[$Zn(OSO_2CF_3)_2L(H_2O)$] (1)

A 15 mL dichloromethane solution of L (0.31 g, 1.0 mmol) was added dropwise to a 15 mL methanol solution of $Zn_2(SO_3CF_3)_2$ (0.36 g, 1.0 mmol) and the system was stirred for 24 h. After filtration, a pale yellow solution was obtained. Slow diffusion into the mother solution of diethyl ether led to colourless crystals which were suitable for X-ray analysis (0.33 g, 49 % based on the salt). Anal. calcd for $C_{23}F_6H_{17}N_3O_7S_2Zn$: C 39.98; H 2.48; N 6.08. Found: C 39.98; H 2.35; N 5.95. TG-DTA determination: H_2O % = 2.55, ZnO % = 13.1; Calc by formula $C_{23}F_6H_{17}N_3O_7S_2Zn$: H_2O % = 2.61, ZnO % = 11.8. ^{1}H NMR (400 MHz, DMSO-d$_6$): δ 7.51 (m, 1.3H), 7.68 ~ 7.78 (m, 3H), 7.97 (s, 2H), 8.29 (s, 2H), 8.44 (d, 2H, J = 6.4 Hz), 8.91 (s, 0.7H), 9.08 (d, 0.7H, J = 7.2 Hz), 9.16 (s, 2H), 9.40 (s, 1.3H). ^{13}C NMR (100 MHz, DMSO-d$_6$): δ 115.92, 119.12, 120.53, 121.19, 122.33, 123.58, 125.53, 127.70, 128.09, 128.23, 129.44, 130.95, 131.16, 135.60, 141.31, 147.38, 147.73, 147.84, 148.80, 149.51, 154.52, 155.24. IR (KBr disc) (cm^{-1}): 3503 (vs), 3062 (w), 1613 (s, $\nu_{\text{pyridyl-H}}$), 1552 (m, $\nu_{\text{aryl-H}}$), 1476 (m, $\nu_{\text{pyridyl-H}}$), 1415 (m), 1262 (vs), 1174 (s), 1036 (s), 886 (w), 795 (w), 767 (m), 644 (s).

[$Zn(OSO_2PhCH_3)_2L$] (2)

40 mL of a dichloromethane solution of L (0.31 g, 1.0 mmol) were added dropwise to 40 mL of

a methanol solution of Zn(p-$SO_3PhCH_3)_2$·$6H_2O$ (0.52 g, 1.0 mmol) and the system was stirred for 24 h. The pale yellow solution thus formed was concentrated and a solid of **2** was obtained by adding 20 mL of diethyl ether. It was separated by filtration, washed with dichloromethane and diethyl ether and dried under vacuum (0.65 g, 90 % yield based on L). Anal. calcd for $C_{35}H_{29}N_3O_6S_2Zn\cdot 2.5H_2O$: C 55.15, H 4.50, N 5.51. Found: C 55.29; H 4.32; N 5.65. ^{1}H NMR (400 MHz, DMSO-d_6): δ 2.26 (s, 6H), 7.07 (d, 4H, J = 8.0 Hz), 7.43 (d, 4H, J = 8.0 Hz), 7.50 (t, 1H, J = 6.2 Hz), 7.67 - 7.76 (m, 3H), 7.90 - 7.98 (m, 2H), 8.27 (t, 2H, J = 7.6 Hz), 8.38 - 8.45 (m, 2H), 8.90 (d, 1H, J = 4.4 Hz), 9.02 (d, 1H, J = 7.6 Hz), 9.07 (s, 1H), 9.18 (d, 1H, J = 8.0 Hz), 9.42 (s, 1H). ^{13}C NMR (100 MHz, DMSO-d_6): δ 20.79, 120.30, 121.17, 123.46, 123.61, 125.46, 127.49, 127.74, 128.26, 129.36, 129.47, 130.89, 131.20, 135.54, 135.64, 137.70, 141.10, 141.36, 145.55, 147.41, 147.73, 147.85, 148.78, 149.51, 154.23, 155.16. IR (KBr disc) (cm^{-1}): 3069 (m), 2924, 1603 (s, $\nu_{pyridyl\text{-}H}$), 1549 (m, $\nu_{aryl\text{-}H}$), 1475 (m), 1415 (m, $\nu_{pyridyl\text{-}H}$), 1263 (s), 1165 (s), 1110 (s), 1207 (w), 1005 (s), 812 (w), 793 (m), 767 (m), 733 (w), 684 (s), 569 (s). Suitable crystals for X-ray analysis were obtained upon dissolution of the white solid in methanol and slow diffusion of diethyl ether. TG-DTA determination of the crystals: ZnO % = 13.1; Calc by formula $C_{35}H_{29}N_3O_6S_2Zn$: ZnO % = 11.4.

[Zn(OCOPh)$_2$L] (3)

A mixture of Zn(OCOPh)$_2$ (0.049 g，0.16 mmol), L (0.050 g, 0.16 mmol) and 20 mL distilled water was sealed in a 25 mL stainless reactor with a Teflon liner and heated at 120 ºC for two days. Colorless crystals of **3** were obtained (0.051 g, 52 % yield based on L). Anal. calcd for $C_{35}H_{25}N_3O_4Zn$: C 68.13; H 4.08; N 6.81. Found: C 68.30; H 4.06; N 6.80. TG-DTA determination: ZnO % = 14.1; Calc by formula $C_{35}H_{25}N_3O_4Zn$: ZnO % = 13.2;. ^{1}H NMR (400 MHz, DMSO-d_6): δ 7.31 (m, 4H), 7.39 (m, 2H), 7.66 (m, 3H), (t, 2H), 7.76 (t, 2H, J = 6.0 Hz), 7.83 (d, 4H, J = 6.8 Hz), 8.27 (m, 4H), 8.89 (d, 2H, J = 3.6 Hz), 8.96 (d, 2H, J = 7.6 Hz), 9.11 (s, 2H). IR (KBr disc) (cm^{-1}): 3059 (m), 1609 (vs, $\nu_{pyridyl\text{-}H}$), 1570 (s, $\nu_{aryl\text{-}H}$), 1477 (m, $\nu_{pyridyl\text{-}H}$), 1414 (s, $\nu_{pyridyl\text{-}H}$), 1372 (vs), 1252 (m), 1167 (w), 1018 (m), 836 (m, $\delta_{Ar\text{-}H}$), 796 (m, $\delta_{Ar\text{-}H}$), 720 (s), 681 (m).

[Zn(p-OCOPhOH)$_2$L] (4)

20 mL of a dichloromethane solution of L (0.12 g, 0.39 mmol) were added dropwise to 20 mL of a methanol solution of Zn(p-OCOPhOH)$_2$·3MeOH·1.5H_2O (0.18 g, 0.39 mmol) in a 100 mL flask

and the mixture was stirred for 24 h. Filtration led to the separation of a white powder of **4** from the mother solution, which was dried in a desiccator (0.14 g, 52 % yield based on L). Anal. calcd for $ZnC_{35}H_{25}N_3O_6{\cdot}2.4H_2O$: C 60.72; H 4.34; N 6.07. Found: C 60.84; H 4.17; N 6.26. TG-DTA: Calc by formula $ZnC_{35}H_{29.8}N_3O_{8.4}$: H_2O % = 6.3, ZnO % = 11.8; Determined: H_2O % = 4.8, ZnO % = 11.2. ^{1}H NMR (400 MHz, DMSO-d_6): δ 6.68 (d, 4H, J = 8.4 Hz), 7.14 (t, 2H, J = 6.8 Hz), 7.29 (t, 1H, J = 6.8 Hz), 7.56 (t, 2H, J = 6.0 Hz), 7.73 - 7.75 (m, 6H), 7.97 (d, 2H, J = 6.8 Hz), 8.46 (d, 2H, J = 6.0 Hz), 8.69 (s, 2H). 8.77 (d, 2H, J = 3.6 Hz), 9.79 (s, 2H, -OH). ^{13}C NMR (100 MHz, DMSO-d_6): δ 114.36, 119.20, 122.22, 126.53, 127.56, 128.85, 130.40, 131.28, 135.01, 139.70, 147.79, 148.54, 148.83, 152.90, 159.79, 170.46, 170.87. IR (KBr disc) (cm^{-1}): 3655 (m, ν_{OH}), 3402 (br, w, ν_{OH}), 3128 (s), 2927 (w, ν_{CH3}), 1602 (vs, br, $\nu_{pyridyl\text{-}H}$), 1554 (vs, $\nu_{aryl\text{-}H}$), 1474 (w, $\nu_{pyridyl\text{-}H}$), 1442 (w, $\nu_{pyridyl\text{-}H}$), 1378 (vs), 1284 (s), 1243 (s), 1162 (m), 1097 (w), 1015 (m), 859 (m, $\delta_{Ar\text{-}H}$), 791 (s, $\delta_{Ar\text{-}H}$), 763 (m, $\delta_{Ar\text{-}H}$), 698 (m), 633 (s). Suitable crystals for X-ray analysis were obtained upon diffusion of the filtrate by diethyl ether.

[Zn(*o*-OCOPhOH)$_2$L] (5)

20 mL of a dichloromethane solution of L (0.12 g, 0.39 mmol) were added dropwise to 20 mL of a methanol solution of Zn(*o*-OCOPhOH)$_2{\cdot}2H_2O$ (0.15 g, 0.39 mmol) in a 100 mL flask and the mixture was stirred for 24 h. Filtration led to the separation of a white powder of **5** from its mother solution, which was dried in a desiccator (0.19 g, 73 % yield based on L). Anal. calcd for $ZnC_{35}H_{25}N_3O_6$: C 64.77; H 3.88; N 6.47. Found: C 64.91; H 3.80; N 6.50. TG-DTA: Calc by formula $ZnC_{35}H_{25}N_3O_6$: ZnO % = 12.5; Determined ZnO % = 13.7. ^{1}H NMR (400 MHz, DMSO-d_6): δ 6.75 (d, 4H, J = 7.6 Hz), 7.28 (t, 2H, J = 7.4 Hz), 7.64 (s, 3H), 7.79 (m, 4H), 8.31 (m, 4H), 8.97 (m, 4H), 9.11 (s, 2H), 13.22 (s, br, 2H, -OH). ^{13}C NMR (100 MHz, DMSO-d_6): δ 116.18, 117.44, 117.72, 120.30, 122.86, 127.32, 128.06, 129.26, 130.61, 130.78, 133.19, 135.66, 140.74, 147.68, 148.68, 148.86, 154.28, 161.15, 173.05. IR (KBr disc) (cm^{-1}): 3749 (w, ν_{OH}), 3446 (br, w, ν_{OH}), 3063 (w), 1602 (vs, br, $\nu_{pyridyl\text{-}H}$), 1483 (s, $\nu_{pyridyl\text{-}H}$), 1413 (w, $\nu_{pyridyl\text{-}H}$), 1390 (s), 1331 (m), 1254 (s), 1159 (m), 1018 (m), 863 (m, $\delta_{Ar\text{-}H}$), 795 (w, $\delta_{Ar\text{-}H}$), 765 (s, $\delta_{Ar\text{-}H}$), 671 (m), 641 (w). Suitable crystals for X-ray analysis were obtained upon diffusion of the filtrate by diethyl ether.

[Zn(*m*-OCOPhOH)$_2$L] (6)

20 mL of a dichloromethane solution of L (0.12 g, 0.39 mmol) were added dropwise to 20 mL of a methanol solution of Zn(*m*-OCOPhOH)$_2$·2H$_2$O (0.15 g, 0.39 mmol) in a 100 mL flask and the mixture was stirred for 24 h. Filtration led to the separation of a white powder of **6** from its mother solution, which was dried in a desiccator (0.22 g, 85 % yield based on L). Anal. calcd for $ZnC_{35}H_{25}N_3O_6 \cdot 0.5H_2O$: C 63.89; H 3.98; N 6.39. Found: C 64.18; H 3.70; N 6.49. ^1H NMR (400 MHz, DMSO-d$_6$): δ 6.77 (d, 2H, J = 7.2 Hz), 7.10 (t, 2H, J = 7.6 Hz), 7.31 (m, 4H), 7.43 (m, 3H), 7.68 (s, 2H), 8.08 (d, 4H, J = 28.4 Hz), 8.82 (t, 6H, J = 37.6 Hz), 9.34 (s, 2H, -OH). ^{13}C NMR (100 MHz, DMSO-d$_6$): δ 116.22, 117.25, 119.58, 120.13, 122.36, 126.75, 127.78, 128.56, 129.07, 130.58, 135.34, 137.77, 140.01, 147.86, 148.69, 148.93, 153.36, 156.86, 170.60. IR (KBr disc) (cm^{-1}): 3402 (m, br, ν_{OH}), 3254 (vs, br, ν_{OH}), 1619 (s, $\nu_{pyridyl\text{-}H}$), 1565 (vs, $\nu_{aryl\text{-}H}$), 1476 (w, $\nu_{pyridyl\text{-}H}$), 1443 (s, $\nu_{pyridyl\text{-}H}$), 1398 (vs), 1350 (s), 1250 (s), 1157 (m), 1113 (m), 1069 (m), 1016 (m), 933 (m), 884 (m, $\delta_{Ar\text{-}H}$), 798 (s, $\delta_{Ar\text{-}H}$), 772 (s, $\delta_{Ar\text{-}H}$), 689 (m), 622 (m), 539 (m), 455 (m). Suitable crystals for X-ray analysis were obtained upon evaporation of the filtrate naturally. Determination of the crystals by TG-DTA: Calc by formula $ZnC_{35}H_{25}N_3O_6$: ZnO % = 12.5; Determined: ZnO % = 13.2.

3.3. Crystal structure determinations

Single crystals of **1-6** were obtained as indicated above. Intensity data were collected using a Bruker AXS-KAPPA APEX II diffractometer with graphite monochromated Mo-Kα (λ 0.71073) radiation. Data were collected using omega scans of 0.5° per frame and full sphere of data were obtained. Cell parameters were retrieved using Bruker SMART software and refined using Bruker SAINT [29] on all the observed reflections. Absorption corrections were applied using SADABS.[29] Structures were solved by direct methods by using the SHELXS–97 package [30] and refined with SHELXL–97.[31] Calculations were performed using the WinGX System–Version 1.80.03.[32] All hydrogens were inserted in calculated positions. Least square refinements with anisotropic thermal motion parameters for all the non–hydrogen atoms and isotropic for the remaining atoms were employed. CCDC 831974, 831975, 831976, 916058, 916059 and 916060 contain the supplementary crystallographic data for this paper. These data can be obtained free of charge from the Cambridge Crystallographic Data Centre via w.ccdc.cam.ac.uk/data_request/cif.

Acknowledgements

The authors are grateful for the financial support from the Foundation for Science and Technology (FCT), Portugal, and its programs (POCI, FEDER funded, Grant No. SFRH/BPD/24691/2005 and Project PEst-OE/QUI/UI0100/2011), the Science Foundation of China (21261002), the Scientific Fund of Guangxi University (X061144) and the Opening Project of Guangxi Key Laboratory of Petrochemical Resource Processing and Process Intensification Technology (K008).

.

References

1 R. Trokowski, S. Akine, T. Nabeshima, *Chem. Commun.*, 2008, 889

2 V. W.-W. Yam, C.-K. Hui, S.-Y. Yu, N. Zhu, *Inorg. Chem.*, 2004, **43**, 812.

3 C. Di Nicola, Effendy, F. Marchetti, C. Pettinari, B. W. Skelton, A. H. White, *Inorg. Chim. Acta*, 2007, **360,** 1433.

4 J. Muller, E. Freisinger, P. Lax, D. A. Megger, F.-A. Polonius, *Inorg. Chim. Acta*, 2007, **360**, 255.

5 S.-S. Zhang, S.-Z. Zhan, M. Li, R. Peng, D. Li, *Inorg.Chem.*, 2007, **46,** 4365.

6 M. Barboiu, L.Prodi, M. Montalti, N. Zaccheroni, N. Kyritsakas, J.-M. Lehn, *Chem. -Eur. J.*, 2004, **10,** 2953.

7 J. S. Field, R. J. Haines, L. P. Ledwaba, R. McGuire Junior, O. Q. Munro, M. R. Low, D. R. McMillin, *Dalton Trans.*, 2007, 192.

8 (a) E. Shikhova, E. O. Danilov, S.Kinayyigit, I. E. Pomestchenko, A. D. Trebulov, F. Camerel, P. Retailleau, R. Ziessel, F. N. Castellano, *Inorg. Chem.*, 2007, **46**, 3038.

9 Y. Fan, Y.-M. Zhu, F.-R. Dai, L.-Y. Zhang, Z.-N. Chen, *Dalton Trans.,* 2007, 3885.

10 P. Du, J. Schneider, W. W. Brennessel, R. Eisenberg, *Inorg. Chem.*, 2008, **47**, 69.

11 C. Hamann, J.-M. Kern, J.-P.Sauvage, *Dalton Trans.*, 2003, 3770.

12 Z. Ma, Y. Xing, M. Yang, M. Hu, B. Liu, M. F. C. Guedes da Silva, A. J. L. Pombeiro, *Inorg. Chim. Acta*, 2009, **362**, 2921.

13 L. Hou, D. Li, *Inorg. Chem. Commun.*, 2005, **8**, 128.

14 J. D. Crowley, A. J. Goshe, I. M. Steele, B. Bosnich, *Chem.-Eur. J.*, 2004, **10**, 1944.

15 a) J. S. Field, C. R. Wilson, O. Q. Munro, *Inorg. Chim. Acta*, 2011, **374**, 197; b) N. W. Alcock, P. R. Barker, J. M. Haider, M. J. Hannon, C. L. Painting, Z. Pikramenou, E. A. Plummer, K. Rissanen, P. Saarenketo, *J. Chem. Soc., Dalton Trans.*, 2000, 1447.

16 (a) Z. Ma, Y. Cao, Q. Li, M. F. C. Guedes da Silva, J. J. R. F. da Silva, A.J.L. Pombeiro, *J. Inorg.*

Biochem, 2010, **104**,704. (b) Z. Ma, B. Liu, H. Yang, Y. Xing, M. Hu and J. Sun, *J. Coord. Chem.*, 2009, **62**, 3314.

17 E. C. Constable, J. Lewis, M.C. Liptrot, P.R. Raithby, *Inorg. Chim. Acta*, 1990, **178**, 47.

18 a) A. Hussain, S. Gadadhar, T. K. Goswami, A. A. Karande, A. R. Chakravarty, *Europ. J. Med. Chem.*, 2012, **50**, 319; b) T. Yutaka, I. Mori, M. Kurihara, J. Mizutani, N. Tamai, T. Kawai, M. Irie, H. Nishihara, *Inorg. Chem.*, 2002, **41**, 7143.

19 a) R. Dobrawa, F. Würthner, *Chem. Commun.*, 2002, 1878; b) T. Dong, M.Lin, S. Chang, C. Ho, S. Lin, L. Lee, *J. Organ. Chem.*, 2007, **692**, 2324; c) P. Song, S. Sun, S. Wang, F. Ma, Y. Xu, X. Peng, *Spectrochim. Acta A: Mol. Biomol. Spectrosc.*, 2011, **81**, 283.

20 M. Liu, Z. Ye, G. Wang, J. Yuan, *Talanta*, 2012, **91**, 116.

21 J. Lombard, R. Boulaouche, D. A. Jose, J. Chauvin, M.-N. Collomb, A. Deronzier, *Inorg. Chim. Acta*, 2010, **363**, 234.

22 H. Padhy, D. Sahu , I-H. Chiang , D. Patra , D. Kekuda , C.-W. Chu, H.-C. Lin, *J. Mater. Chem.*, 2011, **21**, 1196.

23 M. A. Halcrow, *Coord. Chem. Rev.*, 2005, **249**, 2880.

24 C. Hamann, J.-M.Kern, J.-P. Sauvage, *Inorg. Chem.*, 2003, **42**, 1877.

25 É. T. G. Cavalheiroa, M. Ionashiro, G. Marino, S. T. Breviglieri, G. O. Chierice, *J. Braz Chem. Soc.*, 1999, **10**, 65.

26 J. Straszko, M. Olszak-Humienik, J. Możejko, *Thermochim. Acta*, 1997, **292**, 145.

27 Y. Hasegawa, T. Nakagawa, T. Kawai, *Coord. Chem. Rev.*, 2010, **254**, 2643.

28 V. W.-W. Yam, K. K.-W. Lo, *Chem. Soc. Rev.*, 1999, **28**, 323.

29 Bruker, *APEX2 & SAINT. Bruker*, AXS Inc., Madison, Wisconsin, USA, 2004.

30 G. M. Sheldrick, *Acta Crystallogr. Sect. A*, 1990, **46**, 467.

31 G. M. Sheldrick, *Acta Crystallogr. Sect. A*, 2008, **A64**, 112.

32 L. J. Farrugia, *J. Appl. Crystallog.*, 1999, **32**, 837.

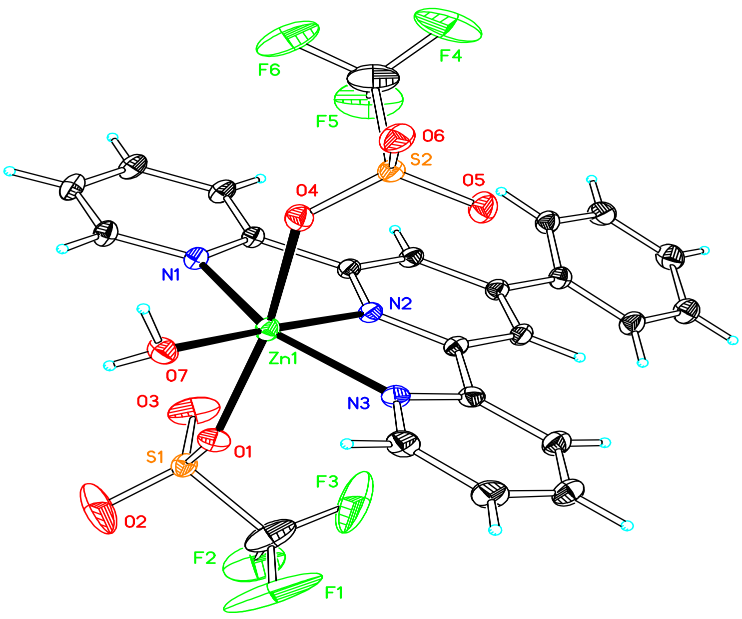

Fig. 1: Thermal ellipsoid plot, drawn at the 30% probability level, of $[Zn(OSO_2CF_3)_2L(H_2O)]$ (**1**) with atomic numbering scheme. Selected bond lengths (Å) and angles (°): Zn1–N1 2.1506(17), Zn1–N2 2.0488(17), Zn1–N3 2.1524(18), Zn1–O1 2.1814(16), Zn1–O4 2.1705(16), Zn1–O7 2.0054(15); N2–Zn1–N1 76.87(6), N2–Zn1–N3 76.48(6), N1–Zn1–N3 153.35(7), O1–Zn1–O4 167.59(6), O1–Zn1–O7 84.28(6), O4–Zn1–O7 83.32(6).

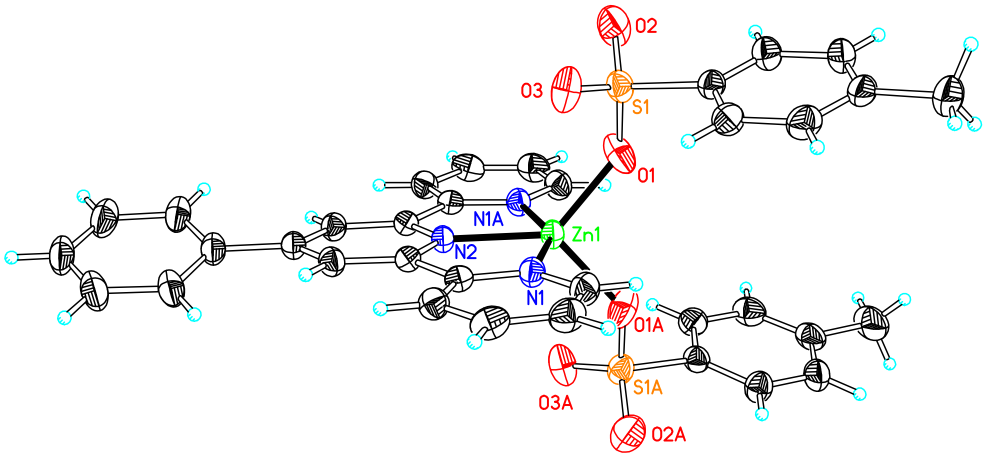

Fig. 2: Thermal ellipsoid plot, drawn at the 30% probability level, of $[Zn(OSO_2PhCH_3)_2L]$ (**2**) with atomic numbering scheme. Symmetry codes: A 1-x, y, 1/2-z. Selected bond lengths (Å) and angles (°): Zn1–N1 2.1570(19), Zn1–N2 2.050(2), Zn1–O1 1.9586(17); N2–Zn1–N1 76.17(5), N1–Zn1–N1A 152.35(10),

O1–Zn1–O1A 98.07(13), O1–Zn1–N1 103.28(8), O1A–Zn1–N1 94.79(8).

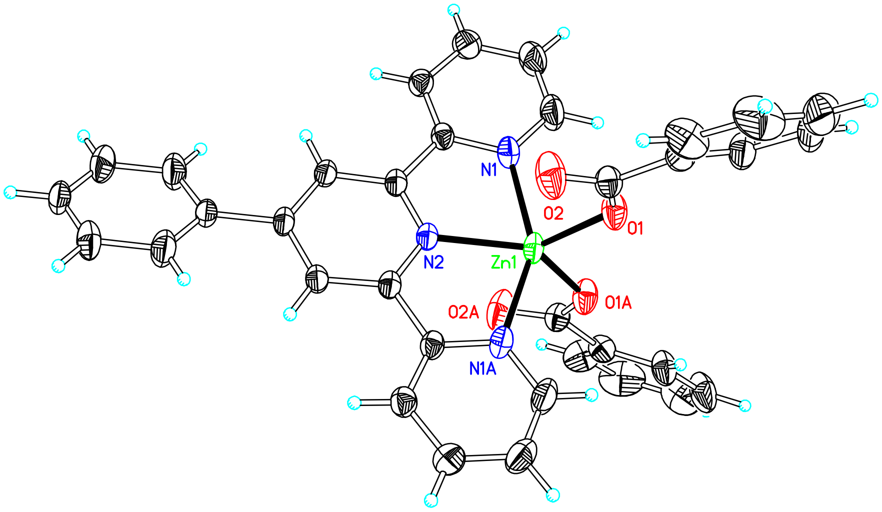

Fig. 3: Thermal ellipsoid plot, drawn at the 30% probability level, of [Zn(OCOPh)$_2$L] (**3**) with atomic numbering scheme. Symmetry codes: A -x, y, 3/2-z. Selected bond lengths (Å) and angles (°): Zn1–N1 2.1780(19), Zn1–N2 2.078(2), Zn1–O1 1.9569(14); N2–Zn1–N1 75.09(4), N1–Zn1–N1A 150.17(9), O1–Zn1–O1A 97.27(8), O1–Zn1–N1 95.60(7), O1–Zn1–N2 131.36(4), O1A–Zn1–N1 104.04(7).

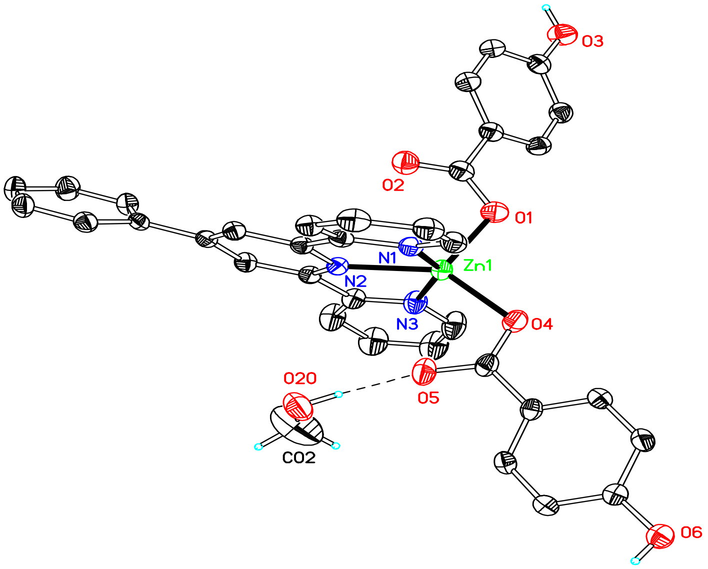

Fig. 4: Thermal ellipsoid plot, drawn at the 30% probability level, of [Zn(p-OCOPhOH)$_2$L]·CH_3OH (**4**·CH_3OH) with atomic numbering scheme. Selected bond lengths (Å) and angles (°): Zn1–N1 2.164(2), Zn1–N2 2.080(2), Zn1–N3 2.202(2), Zn1–O1 1.983(2), Zn1–O4 1.9855(18); N1–Zn1–N2 75.59(8), N1–Zn1–N3 149.01(8), N2–Zn1–N3 74.85(8), O1–Zn1–O4 100.73(8), O1–Zn1–N1 108.85(8), O1–Zn1–N2 119.44(8), O1–Zn1–N3 93.71(9). H atoms at all carbon atoms of the two ligands have been omitted for clarity.

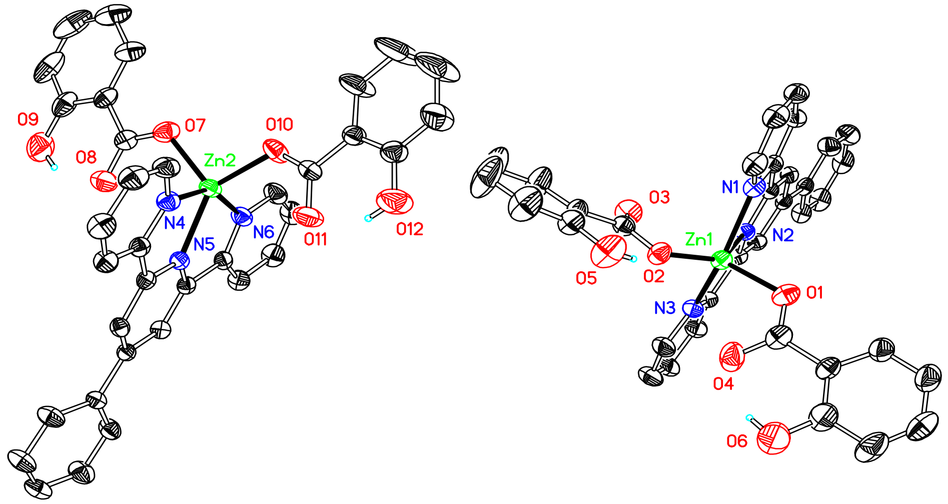

Fig. 5: Thermal ellipsoid plot, drawn at the 30% probability level, of one of the molecules of [Zn(*o*-OCOPhOH)$_2$L] (**5**) with atomic numbering scheme. Selected bond lengths (Å) and angles (°): Zn1–N1 2.210(2), Zn1–N2 2.075(2), Zn1–N3 2.166(2), Zn1–O1 1.990(2), Zn1–O2 1.9841(19); Zn2–N4 2.186(2), Zn2–N5 2.059(2), Zn2–N6 2.171(2), Zn2–O7 1.972(2), Zn2–O10 1.948(2); N1–Zn1–N2 74.70(8), N1–Zn1–N3 148.69(8), N2–Zn1–N3 75.16(8), O1–Zn1–O2 115.48(9), O1–Zn1–N1 93.53(9), O1–Zn1–N2 105.36(9), O1–Zn1–N3 102.40(9), O2–Zn1–N1 93.61(9), O2–Zn1–N2 138.18(8), O2–Zn1–N3 103.28(9). H atoms at all carbon atoms of the two ligands have been omitted for clarity.

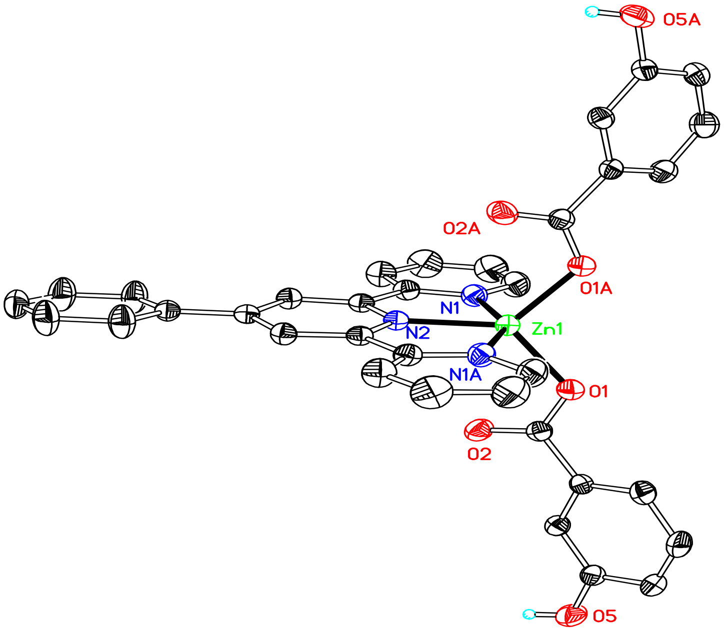

Fig. 6: Thermal ellipsoid plot, drawn at the 30% probability level, of one of the molecules of [Zn(*m*-OCOPhOH)$_2$L] (**6**) with atomic numbering scheme. Symmetry codes: A -x, y, 1/2-z. Selected bond lengths (Å) and angles (°): Zn1–N1 2.1979(16), Zn1–N2 2.0735(17), Zn1–O1 1.9708(12); N1–Zn1–N2 75.35(4), N1–Zn1–N1A 150.70(8), O1–Zn1–O1A 99.54(7), O1–Zn1–N1 106.55(5), O1–Zn1–N2 130.23(3), O1–Zn1–N1A 92.40(5). H atoms at all carbon atoms of the two ligands have been omitted for clarity.

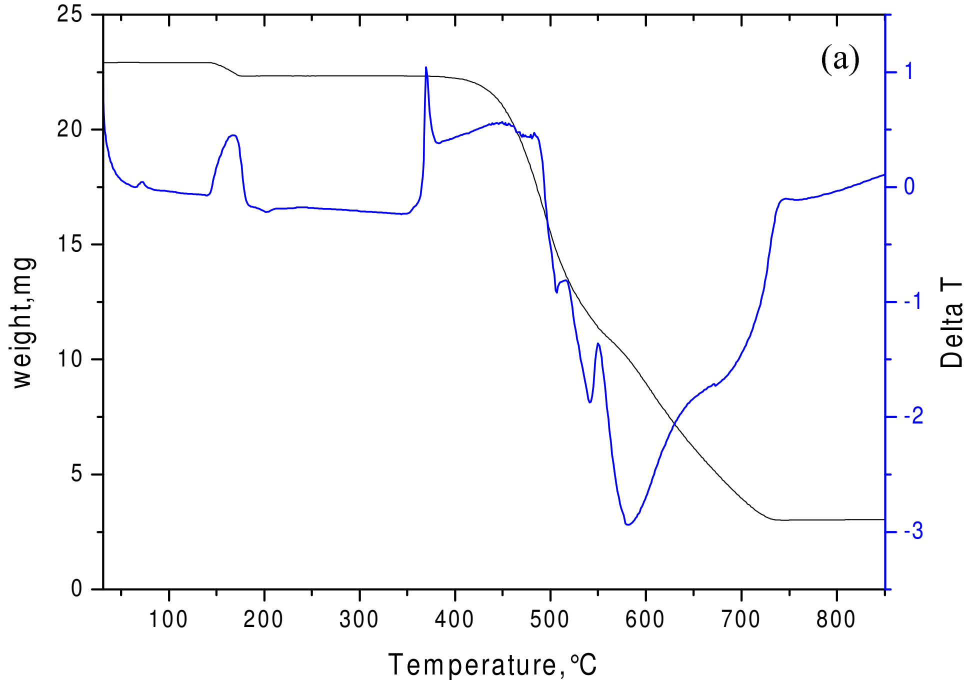

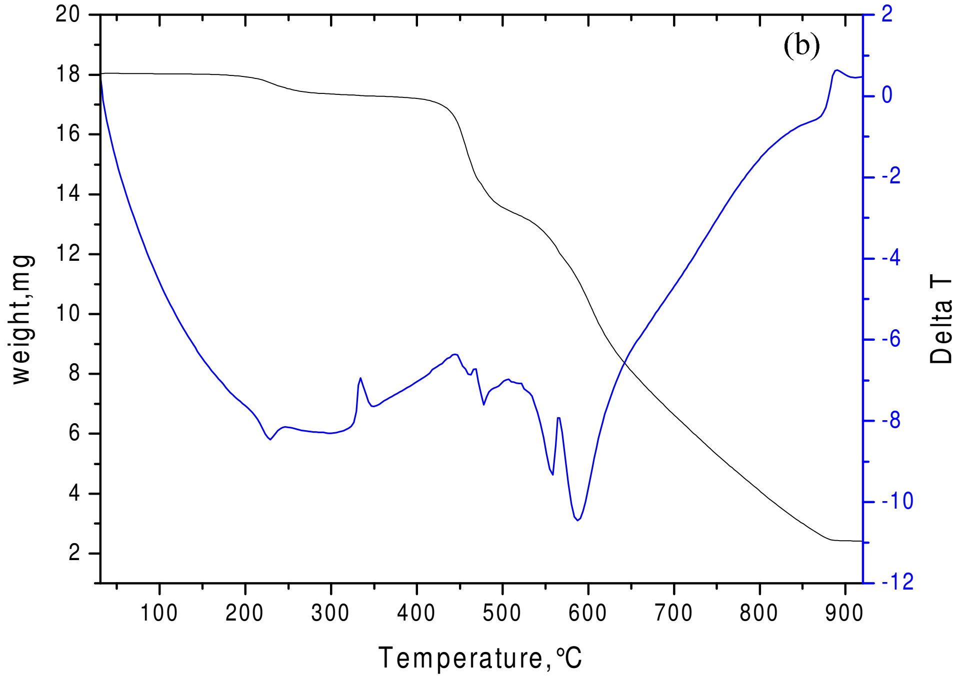

Fig. 7: Thermal analyses (TG and DTA plots) of complexes **1** (a) and **2** (b).

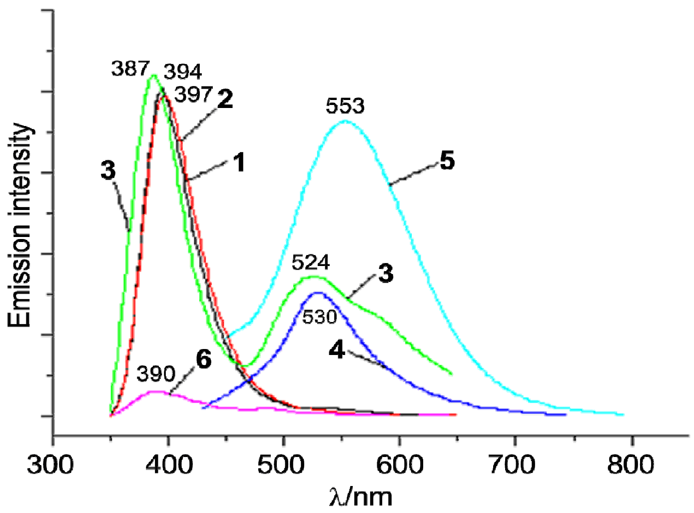

Fig. 8: Solid state emission spectra (excitation at 300 nm for **1**, **2**, **3** and **6**, excitation at 390 nm for **4** and excitation at 410 nm for **5**) of complexes **1** – **6** at room temperature. Sample amounts: 3 mg (**1**, **2**), 25 mg (**3** - **6**).

Table 1 Relevant crystal data for complexes **1** – **6**.

Compounds	**1**	**2**	**3**	**4**·CH_3OH	**5**	**6**
Formula	$C_{23}H_{17}F_6N_3O_7S_2Zn$	$C_{35}H_{29}N_3O_6S_2Zn$	$C_{35}H_{25}N_3O_4Zn$	$C_{36}H_{29}N_3O_7Zn$	$C_{35}H_{25}N_3O_6Zn$	$C_{35}H_{25}N_3O_6Zn$
Formula Weight	690.93	717.14	616.97	681.01	648.97	648.97
Crystal system	Monoclinic	Monoclinic	Monoclinic	Monoclinic	Triclinic	Monoclinic
Space group	*P*2(1)/*c*	*C*2/*c*	*C*2/*c*	*P*2(1)/*c*	*P*-1	*C*2/*c*
a(Å)	11.0686(7)	20.389(4)	19.352(4)	13.007(3)	13.998(2)	16.503(3)
b (Å)	22.0148(13)	13.924(3)	13.626(3)	9.863(2)	14.822(2)	17.021(3)
c (Å)	12.9592(9)	12.196(2)	11.721(2)	26.388(8)	15.489(2)	10.663(2)
α (°)	90	90	90	90	106.615(7)	90
β (°)	117.908(4)	113.21(3)	107.01(3)	110.93(3)	103.451(7)	99.67(3)
γ (°)	90	90	90	90	91.595(7)	90
V (Å^3)	2790.6(3)	3182.2(11)	2955.5(10)	3161.9(14)	2979.6(7)	2952.7(9)
Z	4	4	4	4	4	4
D_{calc} (Mg m^{-3})	1.645	1.497	1.387	1.431	1.447	1.460
μ (mm^{-1})	1.117	0.955	0.875	0.832	0.877	0.885
F(000)	1392	1480	1272	1408	1336	1336
$\theta_{\max}$, $\theta_{\min}$ (°)	28.31, 2.57	28.39, 1.82	28.37, 1.86	27.21, 2.22	28.47, 1.97	28.29, 1.73
Index range h	-12→14	-27→24	-18→25	-16→16	-18→18	-22→21
k	-29→29	-17→18	-16→17	-9→12	-18→19	-22→22
l	-17→17	-14→16	-15→15	-33→33	-20→20	-14→14
Independent reflections	6919	3914	3646	6956	14722	3637
Observed reflections	5801	3104	2949	5248	10316	3096
R_{int}	0.0261	0.0269	0.0302	0.0322	0.0297	0.0204
R	0.0371	0.0372	0.0362	0.0408	0.0476	0.0305
wR	0.0945	0.1126	0.0953	0.1048	0.1144	0.0883
GOF	1.005	1.029	1.000	1.036	1.014	1.024